

## Comprehensive study of pattern formation in relaxational systems

Kevin Wood,<sup>1,2</sup> Javier Buceta,<sup>3</sup> and Katja Lindenberg<sup>1</sup>

<sup>1</sup>*Department of Chemistry and Biochemistry 0340, and Institute for Nonlinear Science, University of California, San Diego, 9500 Gilman Drive, La Jolla, California 92093, USA*

<sup>2</sup>*Department of Physics, University of California, San Diego, 9500 Gilman Drive, La Jolla, California 92093, USA*

<sup>3</sup>*Centre de Recerca en Química Teòrica (CeRQT), Parc Científic de Barcelona, Campus Diagonal—Universitat de Barcelona, Edifici Modular, C/Josep Samitier 1-5, 08028 Barcelona, Spain*

(Received 7 October 2005; published 8 February 2006)

We present a comprehensive study of pattern formation in single-field relaxational systems with field-dependent coefficients. A modulated mean-field theory leads to a form amenable to analysis via the geometric architecture developed in our earlier work for systems that exhibit phase transitions between global steady states [Phys. Rev. E **69**, 011102 (2004)]. We demonstrate that the phase diagrams for these systems are entirely determined by a few geometric properties of the field-dependent relaxational coefficient and the local potential. Numerical simulations support the theoretical predictions.

DOI: [10.1103/PhysRevE.73.022101](https://doi.org/10.1103/PhysRevE.73.022101)

PACS number(s): 05.40.-a, 47.54.-r, 05.10.Gg, 89.75.Kd

The study of the interplay between fluctuations and nonlinearities in spatially extended systems provides insight into the counterintuitive and yet essential role of noise in many ordering transitions [1–8]. In these systems, the intensity of the fluctuations serves as a control parameter dictating the emergence of spatiotemporal structure. While the seminal model of noise-induced phase transitions relied on the collective amplification of short-time instabilities and required the presence of the so-called Stratonovich drift [2], members of another class of relaxational models exhibit such transitions in the absence of short-time instabilities [5,6] and do not require a Stratonovich drift. They rely instead on the existence of a noise-dependent effective equilibrium potential in the steady state whose qualitative behavior is impervious to a particular interpretation of the noise.

Here we extend to pattern formation phenomena our earlier comprehensive study of relaxational models for Ising-like phase transitions between homogeneous states [6]. In particular, we demonstrate via a modulated mean-field approach that the phase diagram of the system can be described by one of only four generalized portraits depending on generic geometric properties of the local potential and field-dependent relaxational functions. Additionally, we complement the theory with numerical simulations which verify its qualitative accuracy.

A generic evolution model of a relaxational space-dependent and time-dependent field  $\varphi_i(t)$  with field dependent coefficients is given in terms of the set of Langevin equations

$$\dot{\varphi}_i(t) = -\Gamma(\varphi_i(t)) \frac{\delta \mathcal{F}(\{\varphi\})}{\delta \varphi_i(t)} + [\Gamma(\varphi_i(t))]^{1/2} \xi_i(t). \quad (1)$$

Here,  $i$  labels a lattice site,  $(\{\varphi\}) \equiv (\varphi_1, \dots, \varphi_N)$  denotes the entire set of fields, and the relaxational function  $\Gamma(\varphi)$  and its square root  $[\Gamma(\varphi)]^{1/2}$  are both positive. The fluctuations  $\xi_i$  are Gaussian white noises with zero mean and correlation functions  $\langle \xi_i(t) \xi_j(t') \rangle = \sigma^2 \delta_{ij} \delta(t-t')$ . The functional  $\mathcal{F}$  consists of a local potential  $V(\varphi)$  and an interaction term, so that  $\delta \mathcal{F} / \delta \varphi_i(t) = -V'(\varphi_i) + \mathcal{L} \varphi_i$ . In our earlier work [6], the opera-

tor  $\mathcal{L}$  was a  $d$ -dimensional nearest neighbor interaction, that is, a discrete version of the Laplacian diffusion operator. Here we will show that if  $\mathcal{L}$  introduces a morphological instability and for appropriate choices of  $V, \Gamma$ , the system undergoes noise-induced phase transitions between disordered, patterned, and multistable phases.

A key ingredient for pattern formation is a competition between length scales. In a nearest neighbor model, there is only one scale (the nearest neighbor distance), and so one needs to modify the interaction to introduce a second scale. We focus on a discrete version of the Swift-Hohenberg operator [9,10],  $\mathcal{L} = -D(k_0^2 + \nabla^2)^2$ , but stress that this specific form is not important, so long as the coupling leads to a morphological instability associated with pattern formation. We focus on the particular discretized form [5,7]

$$\mathcal{L} = -D \left[ k_0^2 + \left( \frac{2}{\Delta x} \right)^2 \sum_{i=1}^d \sinh^2 \left( \frac{\Delta x}{2} \frac{\partial}{\partial x_i} \right) \right]^2, \quad (2)$$

where  $\Delta x$  is the lattice spacing and  $\partial / \partial x_i$  indicates a partial derivative with respect to component  $i$  of the position vector  $\mathbf{r} = (x_1, x_2, \dots, x_i, \dots, x_d)$ . This form arises naturally when one recalls the action of the translation operator  $\exp(\delta x \partial / \partial x) f(x) = f(x + \delta x)$  on any function  $f(x)$ . We can obtain the discrete dispersion relation by applying the operator (2) to a plane wave  $e^{i\mathbf{k} \cdot \mathbf{r}}$ ,

$$\omega(\mathbf{k}) = -D \left[ k_0^2 - \left( \frac{2}{\Delta x} \right)^2 \sum_{i=1}^d \sin^2 \left( \frac{\Delta x}{2} k_i \right) \right]^2. \quad (3)$$

Here  $k_i$  denotes component  $i$  of the wave vector  $\mathbf{k} = (k_1, k_2, \dots, k_i, \dots, k_d)$ .

The most unstable modes are those that maximize  $\omega(\mathbf{k})$ . These modes characterize the underlying spatial regularity indicative of pattern formation. In the continuum, these are the modes with  $k = k_0$ . In the discretized system, the magnitudes  $k^*$  of the most unstable modes are shifted from  $k_0$  and depend on direction. If  $k_0 \Delta x \leq 1$ , then the range of variation of these magnitudes is smaller than 3%. It is, therefore, only a mild approximation to neglect the directional dependence of the solutions as long as one keeps count of the number

of modes that satisfy this condition. The count, detailed in Refs. [5,7], leads to the number  $n(k^*) = [d\pi^{d/2}/\Gamma(d/2+1)](Nk^*/2\pi)^{d-1}$

To capture a spatial structure, we must make an ansatz about the modulated behavior of the field at locations  $\mathbf{r}'$  which are coupled to the focus point  $\mathbf{r}$  by the operator  $\mathcal{L}$  [5] as follows:

$$\varphi_{\mathbf{r}'} = \mathcal{A}(k^*) \sum_{\{k^*\}} \cos[\mathbf{k} \cdot (\mathbf{r} - \mathbf{r}')], \quad (4)$$

where the sum is over wave vectors of magnitude  $k^*$  and all modes are assumed to contribute with equal weight  $\mathcal{A}(k^*)$ . The action of the coupling operator on the ansatz state is detailed in Ref. [5], whence one arrives at the result  $\mathcal{L}\varphi_r = D_1[n(k^*)\mathcal{A}(k^*) - \varphi_r]$ , with

$$D_1 = D \left[ \left( \frac{2d}{(\Delta x)^2} - k_0^2 \right)^2 + \frac{2d}{(\Delta x)^4} \right]. \quad (5)$$

This then leads to an equation for the field that depends only on a generic site index  $\mathbf{r}$  that can simply be dropped

$$\dot{\varphi} = \Gamma(\varphi) \left\{ -\frac{\partial V(\varphi)}{\partial \varphi} + D_1[n^* \mathcal{A}^* - \varphi] \right\} + [\Gamma(\varphi)]^{1/2} \xi(t). \quad (6)$$

We have set  $n(k^*) \equiv n^*$  and  $\mathcal{A}(k^*) \equiv \mathcal{A}^*$ . The noise  $\xi(t)$  is zero-centered, Gaussian, and  $\delta$ -correlated in time,  $\langle \xi(t)\xi(t') \rangle = [\sigma^2/(\Delta x)^d] \delta(t-t')$ . We set  $\Delta x = 1$ .

The mean amplitude  $\mathcal{A}^*$  must be chosen self-consistently to complete the solution of the problem. The stationary probability density for our mean-field stochastic process is

$$\rho_{st}(\varphi; n^* \mathcal{A}^*) = \mathcal{N}[\Gamma(\varphi)]^{(\alpha-1)} \times \exp \left\{ -\frac{2}{\sigma^2} \left[ V(\varphi) + \frac{D_1}{2}(n^* \mathcal{A}^* - \varphi)^2 \right] \right\}, \quad (7)$$

where the normalization constant  $\mathcal{N}$  depends on the amplitude. The constant  $\alpha$  is 0 (1/2) for the Itô (Stratonovich) interpretation of the noise. Self-consistency is implemented with the requirement that  $n^* \mathcal{A}^*$  is the average value of the field at any point in space,

$$n^* \mathcal{A}^* = \int_{-\infty}^{\infty} \varphi \rho(\varphi; n^* \mathcal{A}^*) d\varphi, \quad (8)$$

which is appropriate if the distribution is even in  $\varphi$  and thus  $\mathcal{A}^* = 0$ , or if  $n^* \mathcal{A}^*$  is much larger than the (appropriately phased) combined amplitudes of all the other modes. The latter occurs if there is an instability that leads to the formation of a pattern.

The structure of the mean amplitude problem as given in Eqs. (7) and (8) is formally identical to that obtained for the mean-field problem with diffusive coupling considered in Ref. [6], as is the analytic characterization of the self-consistent solutions. The information provided by the solutions is of course different: in our previous work, the analysis led to the mean-field that characterizes disordered and ordered global phases, whereas here it leads to the amplitude of the least stable modes. There is, therefore, no need to repeat that analysis, and it suffices to reiterate the ‘‘bottom line.’’ We

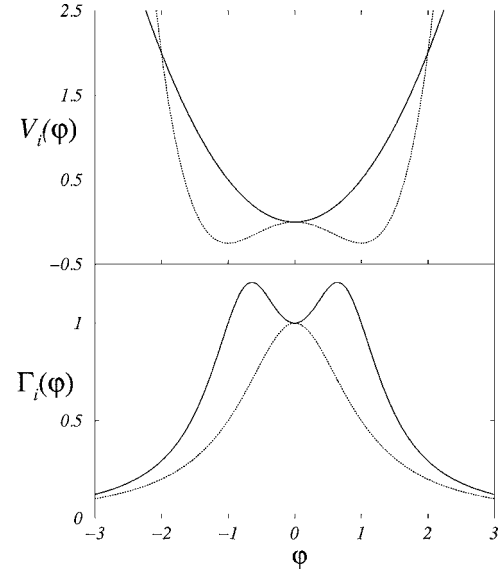


FIG. 1. Generic local potentials  $V_i(\varphi)$  and field-dependent coefficients  $\Gamma_i(\varphi)$  as a function of the field  $\varphi$ . The solid lines are for  $i=1$  and the dotted lines for  $i=2$ .

limit ourselves to potentials  $V(\varphi)$  and relaxation functions  $\Gamma(\varphi)$  of even parity, and furthermore, without loss of generality, require that  $V(0)=0$  and  $\Gamma(0)=1$ .

The entire phase space panorama is captured by considering the four generic combinations obtained by picking one of the two potentials and one of the two relaxation functions illustrated in Fig. 1. While the specific choices

$$V_1(\varphi) = \frac{\varphi^2}{2}, \quad V_2(\varphi) = \frac{\varphi^4}{4} - \frac{\varphi^2}{2}, \quad (9a)$$

$$\Gamma_1(\varphi) = \frac{1 + \varphi^2}{1 + \varphi^4}, \quad \Gamma_2(\varphi) = \frac{1}{1 + \varphi^2} \quad (9b)$$

have been made in the figure, only their general asymptotic behavior and their behavior around the origin is important. The four possible combinations then lead to phase diagrams of the form shown in Fig. 2. These particular ones have been calculated for the specific functions chosen for Fig. 1 with the Itô interpretation in Eq. (7). The Stratonovich interpretation would merely shift the boundaries between phases.

To test the qualitative features of the mean-field analysis via numerical simulations, we look for evidence of the three distinct transitions predicted by our theory: (1)  $O \rightarrow D$  (continuous transition from order to disorder), (2)  $D \rightarrow O$  (continuous transition from disorder to order), and (3)  $D \rightarrow M$  (discontinuous transition from disorder to multistability). The distinction between transitions (1) and (2) is made so as to highlight the drastically different consequences of noise in the various phases. We do not separately consider the  $M \rightarrow O$  transition since it is also marked by the destabilization of the zero amplitude solution and, therefore, closely resembles transition (2). To cover the three transitions, we consider the three representative cases  $[V_2(\varphi), \Gamma_2(\varphi)]$ ,  $[V_1(\varphi), \Gamma_2(\varphi)]$ , and  $[V_1(\varphi), \Gamma_1(\varphi)]$ , which should exhibit (1), (2), and (3), respectively, as noise intensity is increased for an appropriate coupling coefficient  $D_1$  (see Fig. 2). The case

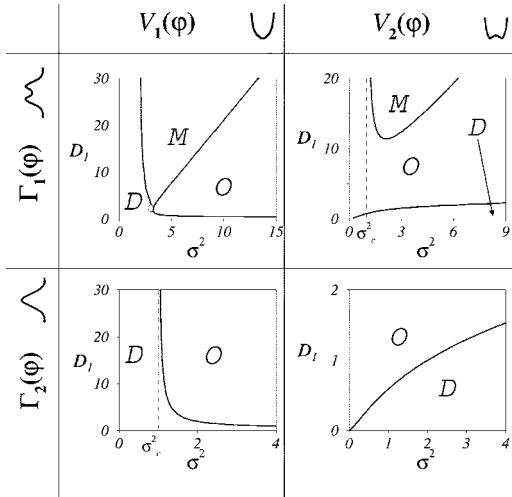


FIG. 2. Mean-field phase diagrams as a function of the local potentials and field-dependent kinetic coefficients illustrated in Fig. 1. The labels  $D$ ,  $O$ , and  $M$  within the diagrams respectively denote disordered, ordered (patterned), and multistable phases (in the latter, both the disordered and ordered phases are stable and can, therefore, in principle, coexist). The small open circle in the phase diagram for  $\Gamma_1$  and  $V_1$  where the three phases merge indicates an isolated singular critical point (*triple point*) where a continuous phase transition between disordered and ordered phases occurs (see Ref. [6]).

$[V_1(\varphi), \Gamma_2(\varphi)]$  was considered in our previous work, but with the Stratonovich interpretation for the noise [5].

We perform our simulations on a lattice of size  $L=N\Delta x=128$  with  $\Delta x=1$ ,  $k_0=1$ , and  $\Delta t=0.005$ . The magnitude of the least stable wave vectors is then  $k^* \sim 1.035$ . With one exception (noted later), we use von Neumann-Dirichlet boundary conditions, that is, the field and its normal derivative are zero at the boundaries. We use an adapted Heun-like algorithm appropriate for an Itô interpretation of the noise [11], and in calculating order parameters, we typically consider time averages obtained once the system has reached a steady state. Our results are essentially identical for different realizations of the noise, so that it is sufficient to present the time-averaged results for any single realization.

There are different ways to characterize pattern formation. For this purpose, we introduce the Fourier transform  $\tilde{\varphi}_k$  of the field  $\varphi_r$ ,  $\tilde{\varphi}_k=(1/N^d)\sum_r \varphi_r \exp(-ik \cdot r)$ . One quantity commonly invoked for the characterization of patterns is the *power spectrum at wave vectors of magnitude  $k$* ,  $S(k)=\sum_{\{k\}} \tilde{\varphi}_k \tilde{\varphi}_{-k}$ , where the sum runs over all modes of magnitude  $k$  (in our discretized system, the sum includes all wave vectors whose magnitude lies in a ring of width  $2\pi/L$  centered on  $k$ ). Another is the *flux of convective heat*,  $J=(1/N^d)\sum_r \phi_r^2$ . The functional relation between these two quantities is simply  $J=\sum_k S(k)$ , where the sum runs over the magnitudes of the modes. One order parameter is  $S(k^*)$  (or, more accurately, the average of  $S(k^*)$  over realizations of the noise but, as noted earlier, we find that different realizations of the noise lead to essentially identical results), which reflects the total contribution of the most unstable modes to the flux of convective heat. Our mean-field theory provides the result  $S(k^*)=n(k^*)\mathcal{A}^2(k^*)$  [8]. Another order parameter is the

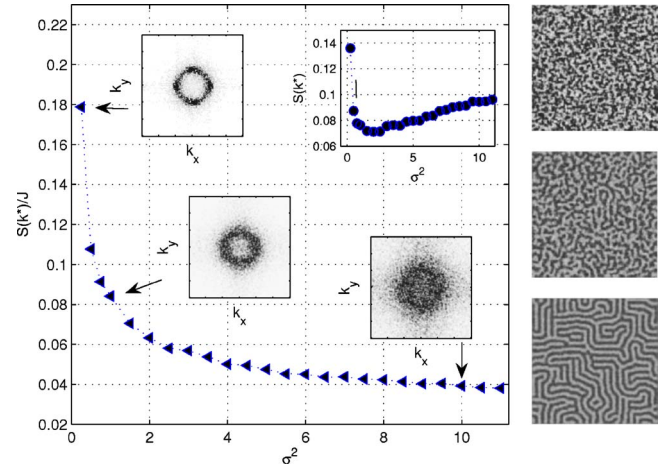


FIG. 3. (Color online) Relative power spectrum for the continuous disordering transition with  $[V_2(\varphi), \Gamma_2(\varphi)]$  and  $D=0.5$ . The snapshots on the right are steady-state configurations for  $\sigma^2=10$ , 1, and 0.25 from top to bottom. Insets show snapshots of the Fourier structure of the field. Upper right inset: power spectrum  $S(k^*)$ .

relative power spectrum  $S(k^*)/J$ , which measures the relative contribution of the least stable modes to the total flux. It provides information on the coherence of the pattern that the simple order parameter  $S(k^*)$  cannot provide. The mean-field theory gives  $J=S(k^*)$  since it only deals with the most unstable modes. A meaningful prediction of  $J$  would require the ability to determine the power spectrum for all wave vector magnitudes. We exhibit both order parameters as obtained from our numerical simulations.

Consider first the case  $(V_2, \Gamma_2)$ . This is the least interesting case since it exhibits patterns only at small noise intensities, with a transition to a disordered state as the noise intensity is increased. Nevertheless, this is a good example to illustrate the information in the two different order parameters and, for that matter, one where the limitations of the mean-field theory become apparent. In the top right inset in Fig. 3, we see the initial decrease of  $S(k^*)$  to zero and the associated disappearance of spatial structure, as predicted. While the mean-field theory does not quantitatively predict the transition parameter values, it does lead to the correct qualitative behavior. The order parameter does not remain at zero after the transition, as the mean-field theory would predict, instead increasing again for larger values of the noise. However, note that as seen in the insets showing the Fourier structure of the spatial configurations, in spite of this increase in the order parameter, the system does not again become ordered with increasing noise because modes other than those of magnitude  $k^*$  become unstable as well. The coherence of the pattern is seen to decrease as the ring of most unstable modes becomes thicker, effectively eliminating the spatial structure visible at low values of the noise. This incoherent configuration consisting of many modes is not captured by the mean-field theory, which is valid only near the bifurcation point. The increasing incoherence with increasing noise is evident in the other order parameter,  $S(k^*)/J$ , which continues to decrease with increasing noise.

Next, consider the case  $(V_1, \Gamma_2)$ , predicted to exhibit a continuous, pattern-forming transition with increasing noise.



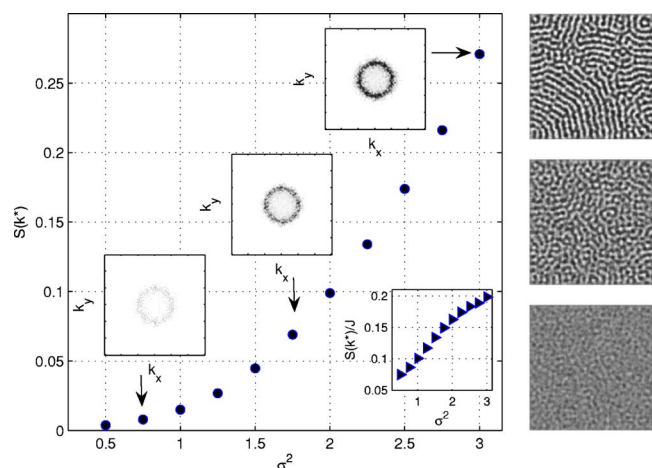


FIG. 4. (Color online) Power spectrum for the continuous disorder-order transition with  $[V_1(\varphi), \Gamma_2(\varphi)]$  and  $D=3$ . The snapshots on the right are the steady-state configurations for  $\sigma^2=3, 1.75$ , and  $0.75$  from top to bottom. Insets: Fourier transforms of the field.

In fact, as evidenced in Fig. 4, increasing the noise for a given value of the coupling constant leads to increasingly visible spatial structure and an ever-intensifying ring of unstable wave vectors. As predicted, the transition is continuous and points to the ordering role of noise in the development of spatial structure.

Finally, we consider the more complex and interesting disorder-multistability transition predicted with the combination  $(V_1, \Gamma_1)$ . Our theory predicts the occurrence of multistability and hysteresis characteristic of a first-order phase transition. To test for the requisite memory of initial conditions, we perform simulations in two directions. In one case, we start from a homogeneous zero-field state and systematically increase  $\sigma^2$ . In the other, we start from the patterned steady state occurring for high noise intensity and decrease  $\sigma^2$ . In each instance, we use the steady state obtained for the previous value of  $\sigma^2$  (either above or below the current one) as the initial state for the subsequent simulation. In order to ensure the timely appearance of a clear pattern, in these simulations we have implemented periodic boundary conditions. Figure 5 demonstrates two clearly different states for the same values of the parameters depending on the initial condition. Hysteresis is also apparent in the marked dependence of  $S(k^*)$  on the initial condition. We have ascertained this same behavior for various realizations of the noise and have also ascertained that hysteresis is only observed in a limited range of parameter values. In particular, for fixed  $D$ , the uniform solution becomes unstable with increasing noise and the system passes into the purely ordered phase.

We have developed a comprehensive theory of noise-induced phase transitions to patterned states in single-field

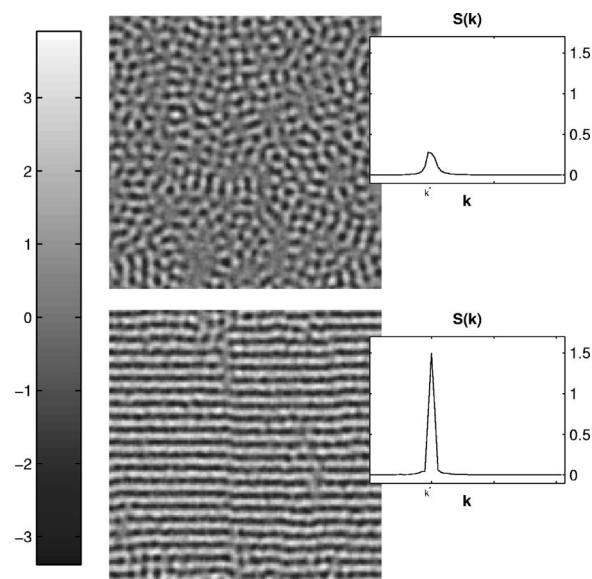


FIG. 5. Snapshots of the field for  $[V_1(\varphi), \Gamma_1(\varphi)]$  that illustrate hysteresis in the discontinuous disorder-order transition with  $D=5$  and  $\sigma^2=3.10$ . The initial condition is uniform in the top panel and a strongly patterned state in the bottom panel. Boundary conditions are periodic. See text for more detailed description of simulation sequence. The insets show the power spectrum  $S(k)$  as a function of  $k$ .

relaxational systems with field-dependent coefficients. Our previous work on this subject focused on a particular system [5], which is here generalized to a broad classification of the geometric properties of the potential function and the relaxational function that lead to one of four possible phase diagrams. Pattern formation requires a length scale competition that we capture via a discrete version of the Swift-Hohenberg coupling. Our comprehensive theory parallels that developed for single-field relaxational systems with nearest neighbor coupling [6]. The theoretical analysis is carried out via a mean-field theory modified from the simplest form by the inclusion of spatial modulation. A linear stability analysis then yields the dispersion relation from which one extracts the most unstable modes. Numerical results confirm the qualitative validity of the theory.

The generosity of R. Kawai in sharing his computational resources is thankfully acknowledged. J.B. gratefully acknowledges the *Ramón y Cajal* program. Support for this work was provided by the National Science Foundation under Grant No. PHY-0354937 and by the Ministerio de Educación y Ciencia (Spain) under Grant No. FIS2005-00457.

- [1] J. García-Ojalvo and J. M. Sancho, *Noise in Spatially Extended Systems* (Springer, New York, 1999).
- [2] C. Van den Broeck *et al.*, Phys. Rev. Lett. **73**, 3395 (1994); C. Van den Broeck *et al.*, Phys. Rev. E **55**, 4084 (1997).
- [3] M. Ibañez *et al.*, Phys. Rev. Lett. **87**, 020601 (2001).
- [4] R. Kawai *et al.*, Phys. Rev. E **69**, 051104 (2004).
- [5] J. Buceta *et al.*, Phys. Rev. E **67**, 021113 (2003).

- [6] J. Buceta and K. Lindenberg, Phys. Rev. E **69**, 011102 (2004).
- [7] J. Buceta *et al.*, Phys. Rev. E **63**, 031103 (2001).
- [8] J. Buceta and K. Lindenberg, Phys. Rev. E **68**, 011103 (2003).
- [9] M. C. Cross and P. C. Hohenberg, Rev. Mod. Phys. **65**, 851 (1993).
- [10] J. Swift and P. C. Hohenberg, Phys. Rev. A **15**, 319 (1977).
- [11] O. Carrillo *et al.*, Phys. Rev. E **67**, 046110 (2003).